$\mathsf{\delta}$ sciendo

Influence of cation order on the dielectric properties of $(1 − x)Pb(Sc_{0.5}Nb_{0.5})O_3$-$xPb(Yb_{0.5}Nb_{0.5})O_3$ ceramics

BARBARA GARBARZ-GLOS[1,2,*], WOJCIECH BĄK[1], MAIJA ANTONOVA[3], ANNA KALVANE[3],
CZESŁAW KAJTOCH[1], PIOTR DULIAN[4]

[1]Institute of Technology, Pedagogical University of Cracow, Podchorążych 2, 30-084 Kraków, Poland

[2]Institute of Technology, The Jan Grodek State University in Sanok, Reymonta 6, 38-500 Sanok, Poland

[3]Institute of Solid State Physics, University of Latvia, Kengaraga 8, Riga LV-1063, Latvia

[4]Faculty of Chemical Engineering and Technology, Cracow University of Technology, Warszawska 24, 31-155 Kraków, Poland

Ceramic lead niobates and their solid solutions $(1 − x)Pb(Sc_{0.5}Nb_{0.5})O_3 − xPb(Yb_{0.5}Nb_{0.5})O_3$ were synthesized by solid state reactions from oxides. The structure of investigated samples was characterized by X-ray diffraction (XRD). Dielectric studies of the ceramics were performed by means of broadband dielectric spectroscopy at the temperature ranging from 600 K to 140 K. For all ceramic samples a diffuse phase transition as well as relaxor ferroelectric behavior were observed.

Keywords: *Pb(Sc0.5Nb0.5)O3; solid solution; dielectric properties; relaxor ferroelectric*

1. Introduction

The wide industrial applications of the $A(BB')O_3$ type compounds (with Pb^{2+} on the A site) are based mainly on the possibility of obtaining the expected structural and dielectric properties by substitution of various transition metal ions on the B site. In the case of complex $Pb(BB')O_3$ ferroelectric materials also chemical distribution of the B site cations and ordering between Sc^{3+} ions and Nb^{5+} ions influences the physical properties of this ceramics [1–3]. This type of material is lead scandium niobate $Pb(Sc_{0.5}Nb_{0.5})O_3$(PSN), investigated for the first time by Smolenskii [4]. Among the possible modifications, the substitution of scandium ions Sc^{3+} with the radius of 0.0745 nm by the ytterbium ions Yb^{3+} with the radius 0.0868 nm in the B site [5] leads to the $(1 − x)Pb(Sc_{0.5}Nb_{0.5})O_{3−x}Pb(Yb_{0.5}Nb_{0.5})O_3$, abbreviated to (1 − x)PSN-xPYN, solid solution. Ceramic ferroelectric materials are now the increasingly important elements of active intelligent systems i.e. those, in which there is a feedback loop between the sensor and actuator and the response of the system is varying and flexible. These materials, in particular PSN with perovskite structure and relaxor ferroelectrics properties, are well known as functional material. The characteristic relaxor behavior relies on a strong frequency and temperature dependence of dielectric response with an extremely slow relaxation below T_m [6, 7]. As a reason for this behavior, many authors pointed out the presence of polar clusters or polar nanoregions in these materials [8, 9]. The relationship between the polar clusters and structural properties of relaxor ferroelectrics is not fully recognized. Therefore, in order to explain the reasons for this phenomenon, several models were proposed [10–12]. The frequency (ν) dependence of temperature T_m corresponding to the dielectric permittivity maxima of relaxor ferroelectrics can be fitted with the Vogel-Fulcher law [13]:

$$\nu = \nu_0 \exp\left(−\frac{E_a}{k_B\left(T_m − T_f\right)}\right) \qquad (1)$$

where ν_0 is the pre-exponential factor, k_B is the Boltzmann constant, E_a is the activation energy

---

*E-mail: barbaraglos@gmail.com

of the polarization flipping mechanism and T_f is freezing temperature of polarization fluctuations.

The scope of the present work was to study the dielectric properties of $(1 - x)$PSN-xPYN (for x from 0 to 0.4) solid solution as a function of composition, temperature and frequency of electric field.

2. Sample preparation

All compositions of $(1 - x)$PSN-xPYN ceramics have been synthesized from reagent grade PbO, Sc_2O_3, Nb_2O_5 and ytterbium carbonate hydrate $Yb_2(CO_3)_3 \cdot 4H_2O$. The homogenizing and grinding of source materials were done in ethanol in an agate ball mill. The obtained slurry was dried at 523 K for 24 h. At first, pure PSN and PYN were prepared and then PSN-PYN solid solution was synthesized from those pure end compounds at 1173 K for 2 h. The single-phase PSN of perovskite structure was prepared by a three-step calcination as follows: the first at 1123 K for 2 h, the second at 1223 K for 2 h and the third at 1573 K for 1 h. The PYN powder was synthesized by two-stage calcination. At the first stage lasting 1 h, $YbNbO_4$ was obtained at 1523 K and at the second-stage, reaction between PbO and $YbNbO_4$ was performed at 1073 K for 2 h. After each calcination, the pellets were immersed in ethanol for 20 h to 24 h, and then ground and dried. The ceramic samples were sintered by hot pressing at 20 MPa from 1 h to 4 h in the temperature range of 1423 K to 1553 K . The highest sintering temperature (1553 K) was used for the PSN sample, and the lowest one (1423 K) for the PYN sample. The obtained ceramic samples had a high density (96 % to 98 % of the theoretical value), a low total porosity (less than 1.0 %) and a negligible water absorption (about 0.02 %).

3. X-ray diffraction measurements

Prior to the X-ray measurements all samples were pulverized in an alundum mortar. The X-ray measurements were performed using Seifert XRD 7 equipment with a horizontal goniometer making use of Ni filtered $CuK\alpha$ radiation. Conditions of the measurements were as follows: the range

of angles $2\theta = (10° - 90°)$ with $0.02°$ interval, with the step of counting time 2 s. The results of the measurements are presented in Fig. 1. X-ray powder diffraction of the samples at room temperature showed a single phase of perovskite type structure.

Its symmetry changed from a rhombohedral distortion of the cubic lattice with parameters: a = 0.4083 nm and $\alpha = 89.96°$ for pure PSN to a pseudomonoclinic (a = 0.4120 nm) perovskite phase for the PYN compositions, taking the form of an interstitial solid solution. The values of lattice parameters increased with increasing ytterbium content in the solid solution (in Fig. 1, shifting the diffraction peaks towards lower angles in comparison to the lead scandium niobate PSN with increasing PYN content is observed). Nevertheless, changes in the α angle values are small, and amount to $89.98°$, $89.99°$ for 0.8PSN-0.2PYN and 0.6PSN-0.4PYN, respectively.
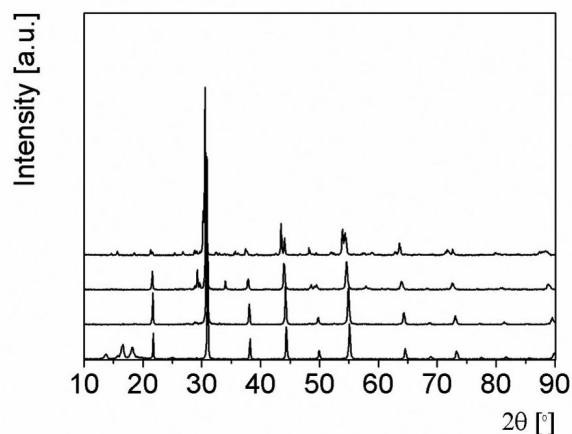

Fig. 1. Room temperature X-ray diffraction profiles for $(1 - x)$PSN-xPYN samples.

4. Dielectric properties measurements

Dielectric measurements of $(1 - x)$PSN-xPYN ceramic samples were performed using an Alpha-AN high performance frequency analyzer (Novocontrol Technologies) combined with Quatro Cryosystem for the temperature control. The samples with silver electrodes were fixed between two metal electrodes in a sample holder and placed

in a cryostat. The measurements were performed in the temperature range from 140 K to 600 K. The frequencies varied from 0.1 Hz to 10 MHz at an applied voltage of 1 V. Before the measurements the samples were heated to release any strains both internal and from the electrode surface. Nitrogen gas was used as a heating and cooling agent.
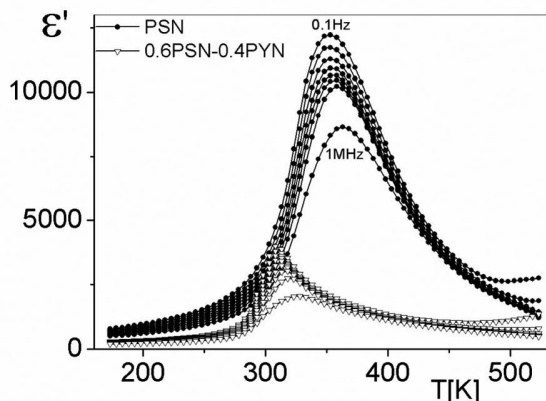

Fig. 2. The dependence of the real part of dielectric permittivity on temperature for PSN and 0.6PSN-0.4PYN samples.

For PSN and 0.6PSN-0.4PYN ceramic samples the temperature dependence of the real part of dielectric permittivity $\epsilon'(T)$ is presented in Fig. 2. The run of the $\epsilon'(T)$ curves testifies to the diffuse phase transitions. For all applied frequencies, the maximum values of the $\epsilon'(T)$ do not occur at the same temperature. The increase in frequency results in a shift of the temperature T_m, which corresponds to the maximum of dielectric permittivity causing a strong dispersion of ϵ'_m. Simultaneously, the values of the $\epsilon'_m(T)$ maximum decrease. Fig. 3 presents the dependences of $\epsilon'(T)$ at the frequency ranging from 0.1 Hz to 10 MHz for 0.8 PSN-0.2PYN sample.

Such behavior is typical of relaxors and can be related to the formation and reorientation of polar nanoregions (PNRs). A significant contribution to the formation of PNRs has the electronic subsystem, especially the localization of charge carriers on the defects in the temperature close to phase transition. The average size of PNRs increases with decreasing temperature (saturates
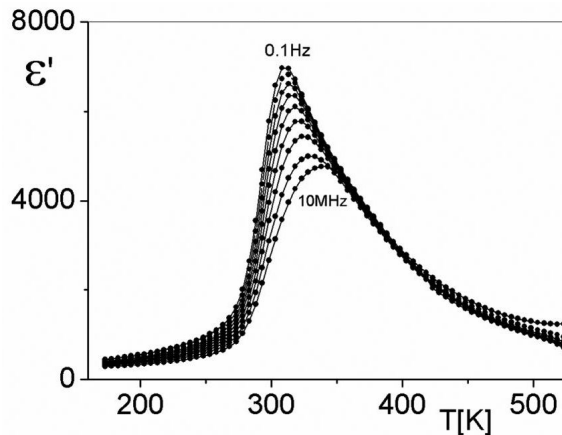

Fig. 3. The dependence of the real part of dielectric permittivity on temperature for 0.8 PSN-0.2 PYN sample.

below T_m) and the dynamics of polar nanoregions extremely decreases. At the freezing temperature T_f, the PNRs become frozen into a nonergodic state, the relaxation time becomes infinite and the thermally activated reorientation of dipoles responsible for polarization becomes impossible [8, 9, 14]. The freezing temperature T_f and the activation energy of the polarization flipping mechanism E_a for this sample were determined with the use of Vogel-Fulcher relationship (Fig. 4). The values of T_f and E_a for 0.8 PSN-0.2 PYN are 210 K and 0.75 eV, respectively. The effect of cation arrangement on relaxor behavior of ferroelectrics appears to be particularly strong. The sensitivity of material properties to cation arrangement through control of ordering can be used to develop new classes of electroceramics [11, 15, 16].

The increase of ytterbium content (PYN) in the examined $(1 - x)$PSN-xPYN solid solution, at first caused a shift of the phase transition temperature towards lower temperatures for x up to 0.4, and then an increase up to 570 K (Fig. 5). Simultaneously, an increase of the PYN content in the $(1 - x)$PSN-xPYN caused a systematic decrease in ϵ'_m values.

Numerous studies [9, 17–19] point out that the chemical composition plays a key role in determining the balance of long ranged Coulomb
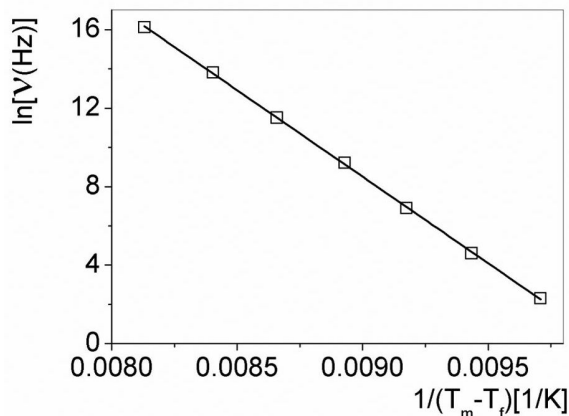
Fig. 4. Logarithm of the measurement frequency as a function of inverse of temperature corresponding to the maximum value of the real part of permittivity for 0.8 PSN-0.2 PYN sample.
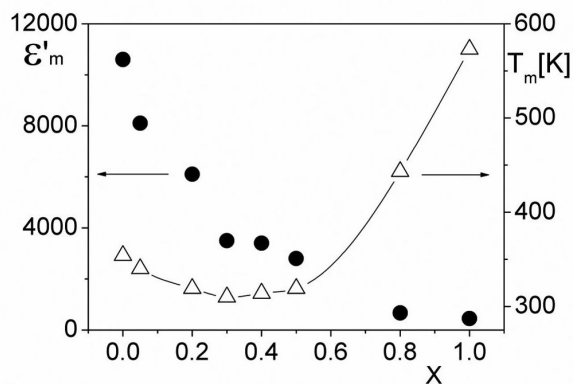

Fig. 5. Maximum of real part of dielectric permittivity ϵ_m' and corresponding temperature T_m for various PYN contents.

interactions, responsible for the appearance of the ferroelectric state, and repulsive short range interactions, whose dominance decides about the stability of non-polar structure, are the essential factor for describing the phase transition mechanism. Changes in the degree of long-range compositional order and its influence on the ferroelectric/antiferroelectric character of the phase transition, can be explained on the basis of the cation-anion bonds model [9, 17, 19]. According to this model, the temperature of phase transition can be assigned to the change in the size of oxygen octahedra surrounding "ferroelectric" ions in

the $A(BB')O_3$ perovskite structure. If the average diameter of the oxygen octahedra around the B, B′ cations decreases, the short-range restoring forces increase, and the ferroelectric-paraelectric transition temperature is decreased; in contrast the antiferroelectric-paraelectric transition temperature increases [19, 20].

5. Conclusions

The $(1 - x)$PSN-xPYN solid solutions were obtained by a conventional ceramic method. The dielectric studies show that the $(1 - x)$PSN-xPYN with ytterbium content from x = 0 to x = 0.4 is a relaxor ferroelectric. Such behavior is a result of different valences of substituted ions in both cationic sub-lattices. The strong dispersion of the dielectric permittivity maximum is observed. The Vogel–Fulcher relationship has been used to describe the frequency dependence of dielectric permittivity maxima (T_m). The obtained results clearly indicate that incorporation of ytterbium to the $(1 - x)$PSN-xPYN successfully decreased the phase transition temperature (to x = 0.4) and then increased it up to x = 1. The increase of the ytterbium content (above x = 0.4) in the $(1 - x)$PSN-xPYN caused a decrease in ϵ_m' values and the ceramic samples exhibited antiferroelectric-paraelectric phase transition.

References

[1] PARK Y., CHO K., *J. Am. Ceram. Soc.*, 83 (2000), 135.
[2] DAMBEKALNE M., *Ferroelectrics*, 371 (20080, 21.
[3] BORMANIS K., *J. Eur. Ceram. Soc.*, 24 (2004), 1557.
[4] SMOLENSKII G.A., ISUPOV V.A., AGRANOVSKAYA A.I., *Sov. Phys. Solid State*, 1 (1959), 10.
[5] SHANNON R.D., *Acta Crystallogr. A*, 32 (1976), 751.
[6] GARBARZ-GLOS B., *Ferroelectrics*, 485 (2015), 173.
[7] MACUTKEVIC J., *Phys. Rev. B*, 83 (2011), 184301.
[8] MANLEY M.E., *Nature Comm.*, 5 (2014), 3683.
[9] BOKOV A.A., YE Z.G., *J. Mater. Sci.*, 41 (2006), 31.
[10] UCHINO K., *Relaxor Ferroelectric-Based Ceramics,* in: *Advanced Piezoelectric Materials: Science and Technology*, Woodhead Publishing Limited, Oxford, 2017, p. 127.
[11] BURTON B.P., COCKAYNE E., WAGHMARE U.V., *Phys. Rev. B*, 72 (2005), 064113.
[12] KLEEMANN W., *J. Mater. Sci.*, 41 (2006), 129.
[13] FULCHER G.S., *J. Am. Ceram. Soc.*, 8 (1925), 339.
[14] PIRC R., BLINC R., *Phys. Rev. B*, 76 (2007), 020101.

[15] Rieth M., Schommers W., *Handbook of Theoretical and Computational Nanotechnology*, American Scientific Publishers 2006.

[16] Rabe K. M., Ahn C.H., Triscone J.-M., *Physics of Ferroelectrics: A Modern Perspective*, Springer Berlin Heidelberg, 2010.

[17] Kirillov S.T., *Ferroelectrics*, 100 (1989), 121.

[18] Sakhnenko V.P., *Kristallografiya*, 17 (1972), 316.

[19] Bokov A.A., *JETP*, 84 (1997), 994.

[20] Shonov V.Yu., Raevskii I.P., *Techn. Phys.*, 3 (1999), 285.